Electronic Supplementary Material (ESI) for ChemComm.

Supporting Information

Diarylboryl-phenothiazine Based Multifunctional Molecular Siblings

Kalluvettukuzhy K. Neena, Pagidi Sudhakar, Kumbhar Dipak and Pakkirisamy Thilagar*

Department of Inorganic and Physical Chemistry,

Indian Institute of Science, Bangalore-560012, Karnataka, India.

Ph. No. +91-080-2293 3353 Fax: +91-80-2360 1552.

E-mail:thilagar@ipc.iisc.ernet.in

Experimental Section

Materials

The chemicals were purchased from commercial suppliers (Aldrich, USA; Merck, Germany; SDFCL, India) and used as received, unless otherwise mentioned. Standard Schlenk-line technique was used for reactions. THF was dried over sodium and distilled out under argon atmosphere.

Methods

^{1}H, ^{11}B and ^{13}C NMR spectra were recorded at 25 °C on a Bruker Avance 400 MHz NMR Spectrometer operating at a frequency of 400 MHz for ^{1}H, 376.5 MHz for ^{11}B and 100 MHz for ^{13}C. ^{1}H NMR spectra were referenced to TMS (0.00 ppm) as an internal standard. Chemical shift multiplicities are reported as singlet (s), doublet (d), triplet (t), quartet (q), and multiplet (m). ^{13}C resonances were referenced to the $CDCl_3$ signal at ~77.67 ppm. ^{11}B NMR chemical shift values were referenced to the external standard boron signal of $BF_3 \cdot Et_2O$. High resolution mass spectra (HRMS) were recorded on a Micromass Q-ToF High Resolution Mass Spectrometer by electrospray ionization (ESI) method. Electronic absorption spectra and fluorescence emission spectra were recorded on a SHIMADAZU UV-2600 spectrophotometer and Horiba JOBIN YVON Fluoromax-4 spectrometer, respectively. The time-resolved fluorescence (TRF) decay measurements were carried out at a magic angle using a nanosecond diode laser based time correlated single photon counting (TCSPC) fluorescence spectrometer from IBH, UK. Solutions of all the compounds for spectral measurements were prepared using spectrophotometric grade solvents, microbalance (± 0.1 mg precision) and standard volumetric glass wares. Quartz cuvettes with sealing screw caps were used for the solution state spectral measurements. Single-crystal X-ray diffraction studies were carried out with a Bruker SMART APEX diffractometer equipped with 4-axis goniometer for compound **1** and Oxford Xcalibur (Mova) diffractometer equipped with an EOS CCD detector for compound **2**. The data were integrated using SAINT, and an empirical absorption correction was applied with SADABS[1]. The structures were solved by direct methods and refined by full matrix least-squares on F^2 using SHELXTL software. Density functional theory (DFT) calculations were done using B3LYP functional with 6-31G(d) basis set as incorporated in *Gaussian 09* package for all the atoms, mixing the exact Hartree-Fock-type exchange with Becke's exchange functional and that proposed by Lee-Yang-Parr for

the correlation contribution.[2] The optimized structures and the frontier molecular orbitals (FMOs) were viewed using *Gaussview5.0.* Thermo-Gravimetric Analysis (TGA) curves of compounds were collected in a NETZSCH TG 209 F1 apparatus at a heating rate of 10 °C/min under argon atmosphere. TEM images of compounds were recorded on a 200 kV JEOL FETEM, the samples were prepared drop-casting the respective solutions on copper grid and then drying for overnight. Delayed Light Scattering (DLS) measurements were carried out in Brookhaven Zeta plus Instrument and data were analyzed using ZetaPlus Particle Sizing Software Version 5.23.

Synthesis

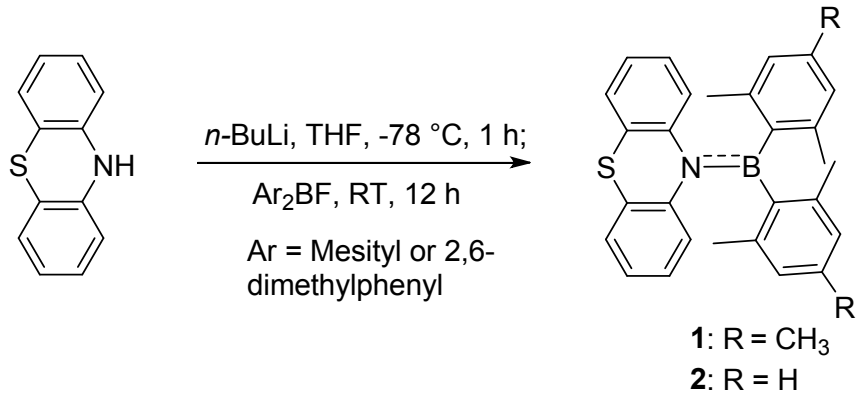

Scheme S1: Synthesis of compounds **1** and **2**

Synthesis of 10-(dimesitylboryl)-phenothiazine (1)

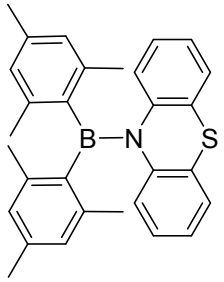

A 1.6 M solution of *n*-BuLi (1.6 M, 3.01 mmol) in hexane was added drop wise to THF solution of phenothiazine (500 mg, 2.51 mmol) at around -78 °C under stirring condition. A solution of dimesitylboronfluoride (800 mg, 3.01 mmol).in THF was added to the reaction mixture after 45 min at the same temperature. The reaction mixture was allowed to warm to room temperature and stirring continued for another 5 hours. Volatile organic solvents were removed under reduced pressure. The resultant residue was dissolved in dichloromethane (DCM) and extracted with water (3 x 100 mL). The combined organic layer was dried over Na_2SO_4 and removal of organic volatiles under reduced pressure and then compound was purified by column chromatography on silica gel using hexane as eluent and

further recrystallized by slow evaporation of dichloromethane solution to produce off-white color crystals. Yield: 89 % (1.00 g). ^{1}H NMR (400 MHz, $CDCl_3$, 25 °C): δ (ppm) 2.19 (s, 6H), 2.38 (s, 12 H), 6.66 (br s, 4H), 6.86-6.90 (m, 2H), 6.96- 7.00 (m, 2H), 7.15-7.17 (m, 2H), 7.25-7.26 (m, 2H) .^{11}B NMR (376.5 MHz, $CDCl_3$, 25 °C): δ (ppm) 49.20. ^{13}C NMR (100 MHz, $CDCl_3$, 25 °C): δ (ppm) 21.0, 24.1, 125.2, 125.4, 126.5, 127.2, 128.1, 129.9, 137.1, 138.7, 140.6, 143.5. HRMS (ESI-MS, positive ion mode): calcd. for $C_{30}H_{30}BNS$ 447.4419 Da, observed 470.2090 Da $(M+Na)^+$.

Synthesis of 10-(bis(2,6-dimethylphenyl)boryl)-phenothiazine (2)

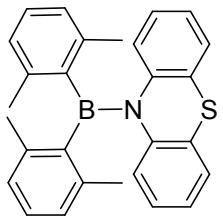

Compound **2** was prepared by following the similar procedure described for compound **1**. The quantities involved and characterization data are as follows: Phenothiazine (500 mg, 2.51 mmol), *n*-BuLi (1.6 M, 3.01 mmol), bis(2,6-dimethylphenyl)boronfluoride (720 mg, 3.01 mmol). The compound was purified by column chromatography on silica gel using hexane as eluent and further recrystallized by slow evaporation of dichloromethane solution to produce off-white color crystals. Yield: 95 % (1.00 g). ^{1}H NMR (400 MHz, $CDCl_3$, 25 °C): δ (ppm) 2.44 (S, 12H), 6.84- 6.88 (m, 6H), 6.97- 7.04 (m, 4H), 7.15- 7.17 (d, 2H), 7.26- 7.28 (d, 2H). ^{11}B NMR (376.5 MHz, $CDCl_3$, 25 °C): δ (ppm) 50.88. ^{13}C NMR (100 MHz, $CDCl_3$, 25 °C): δ (ppm) 24.6, 125.7, 125.8, 126.8, 127.5, 127.6, 128.2, 130.3, 141.1, 143.6. HRMS (ESI-MS, positive ion mode): calcd for $C_{28}H_{26}BNS$ 419.1879 Da, observed 442.1777 Da $(M+Na)^+$.

NMR Spectral Characterizations

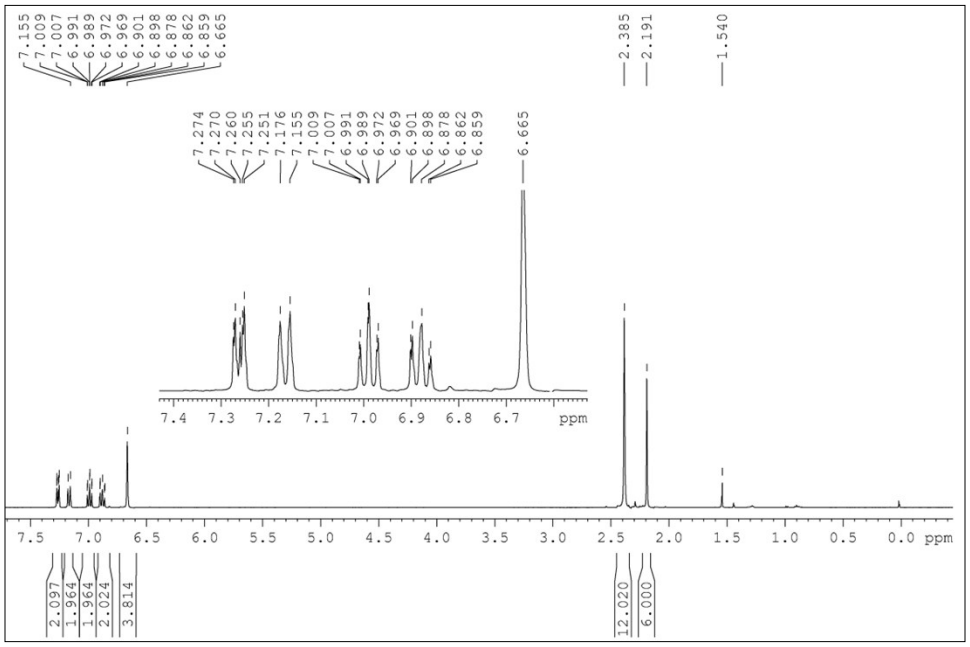

Figure S1: ^{1}H NMR spectrum of compound **1 (**δ= 1.54 ppm corresponds to H_2O in $CDCl_3$, and inset shows the expanded ^{1}H NMR spectrum of 1 in the region 7.40-6.60 ppm)

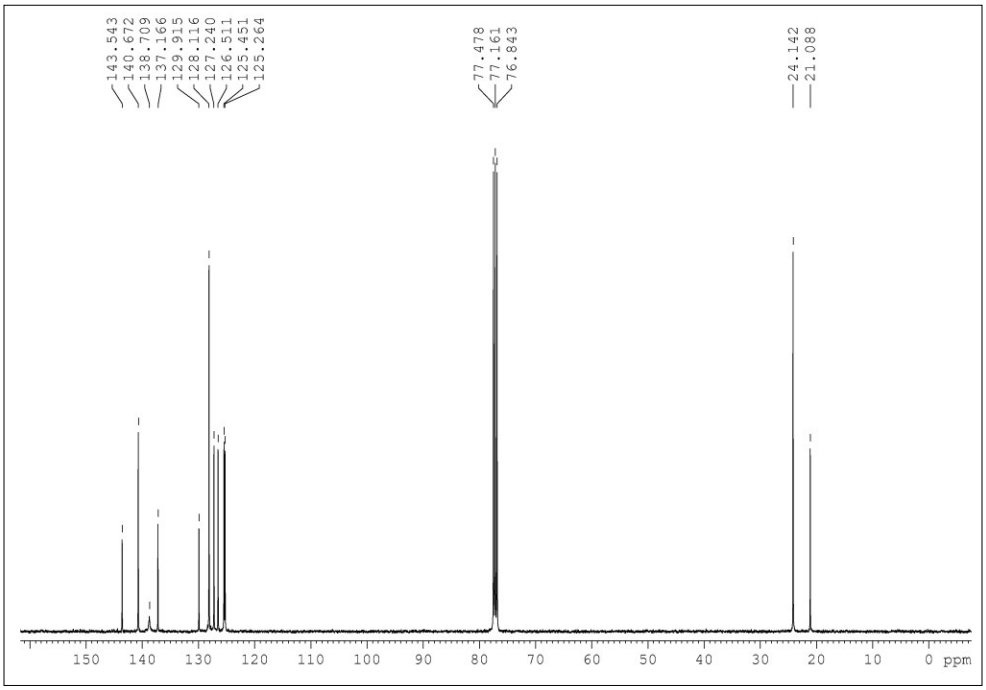

Figure S2: ^{13}C NMR spectrum of compound **1**

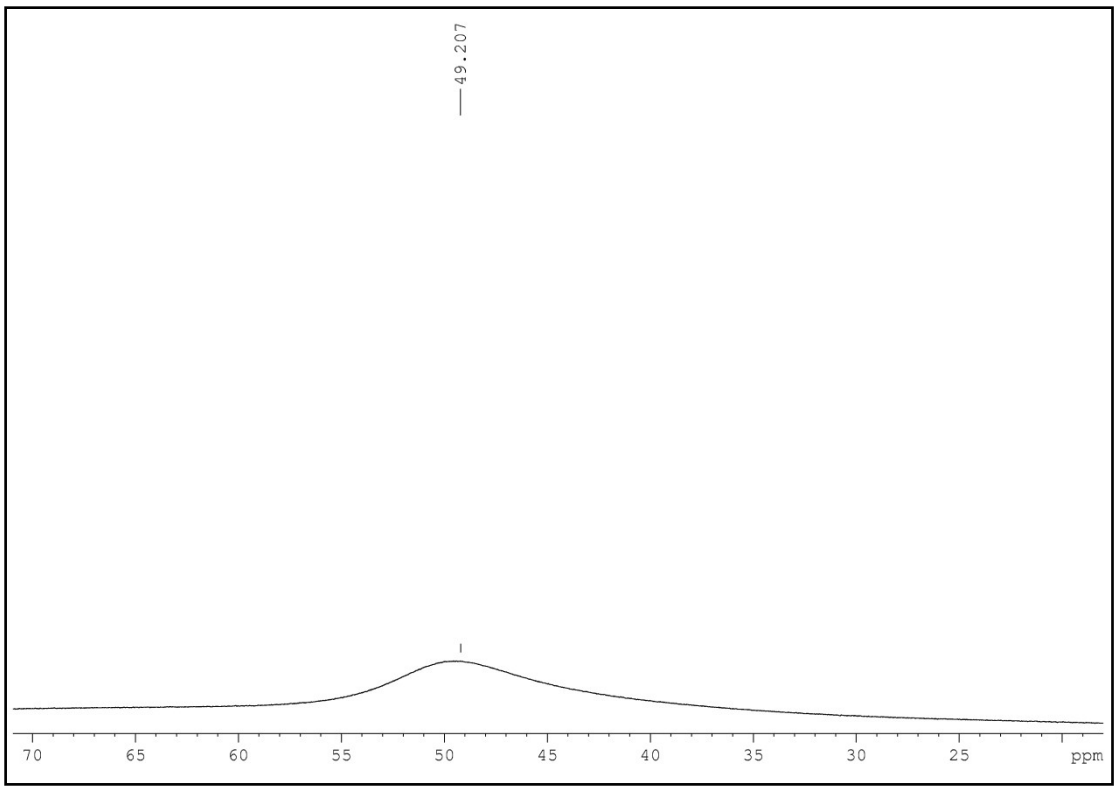

Figure S3: ^{11}B NMR spectrum of compound **1** (the peak at 49.20 ppm corresponds to the ^{11}B NMR resonance of compound **1**)

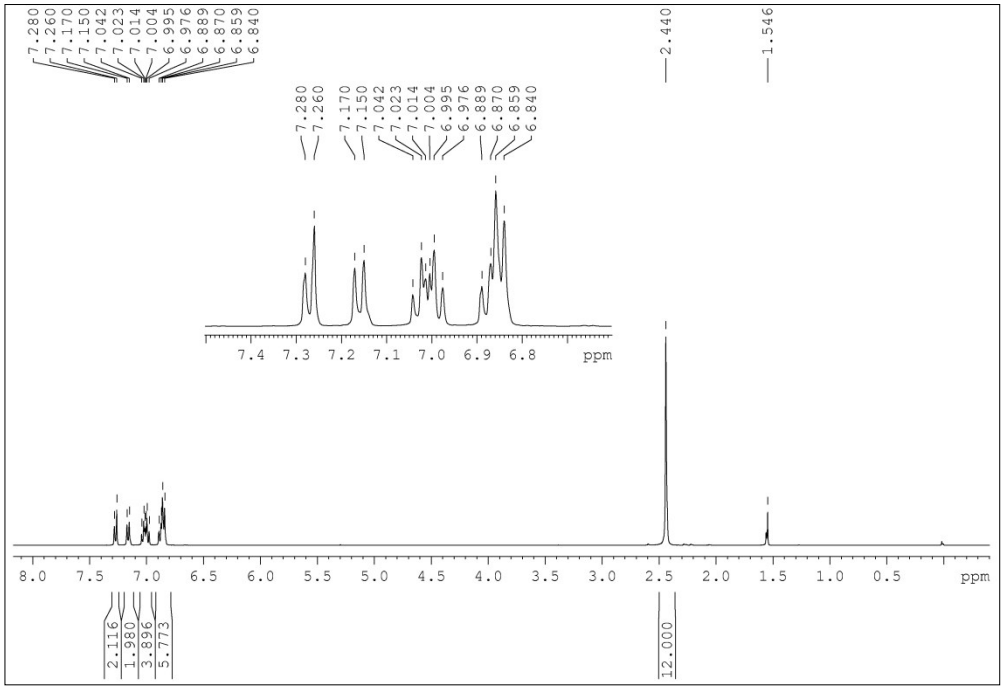

Figure S4: ^{1}H NMR spectrum of compound **2** (δ= 1.54 ppm corresponds to H_2O in $CDCl_3$ and inset shows the expanded ^{1}H NMR spectrum of 1 in the region 7.40-6.70 ppm)

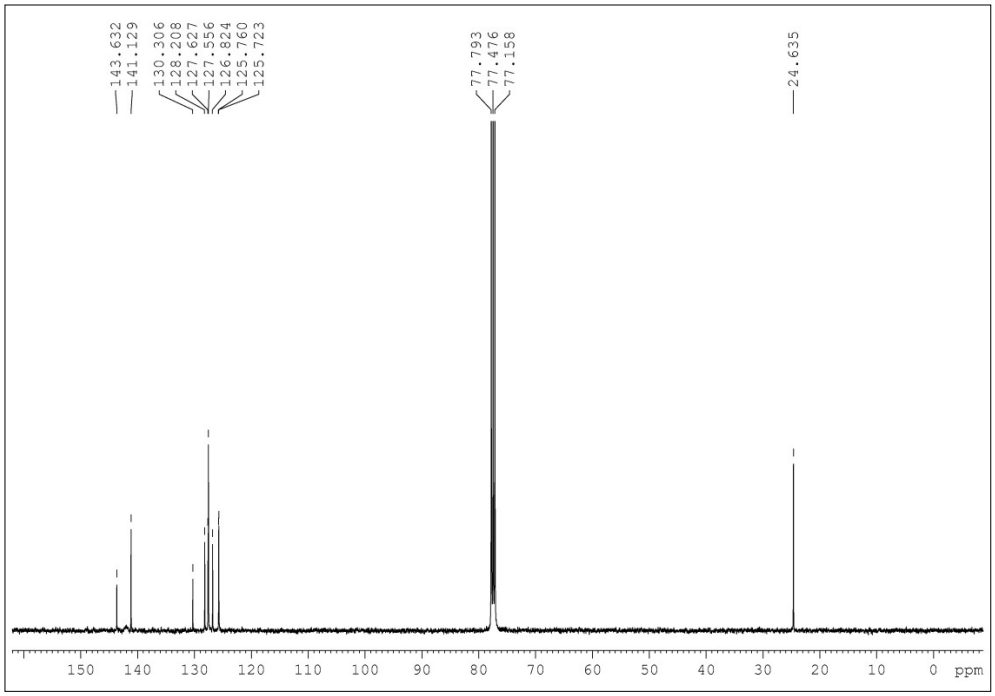

Figure S5: ^{13}C NMR spectrum of compound **2**

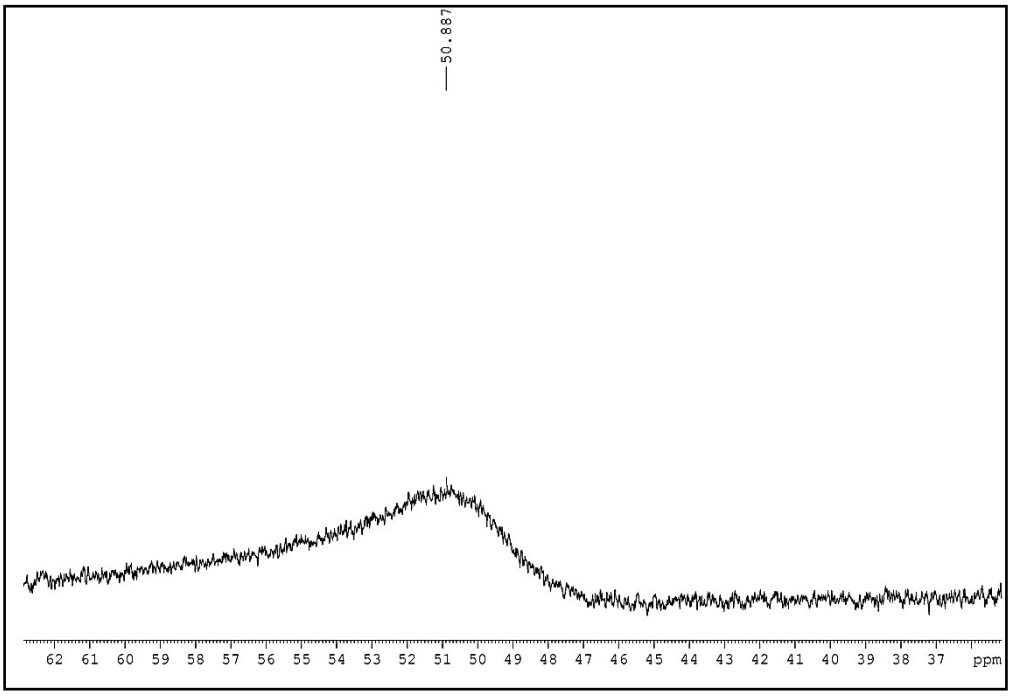

Figure S6: ^{11}B NMR spectrum of compound **2** (the peak at 50.88 ppm corresponds to the ^{11}B NMR resonance of compound **2**)

Mass Spectral Characterization

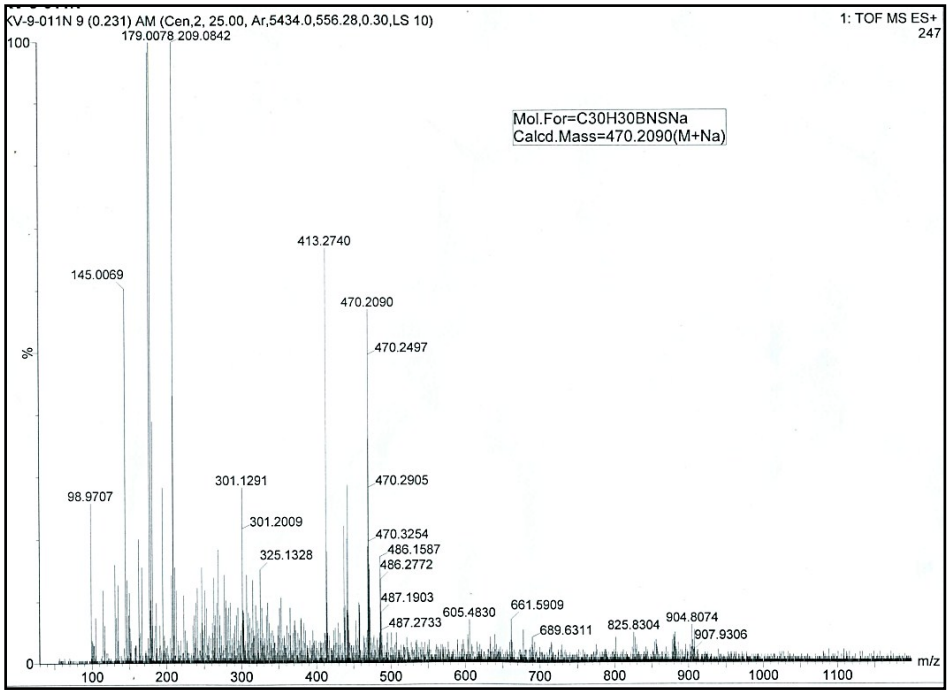

Figure S7: HRMS of compound **1**

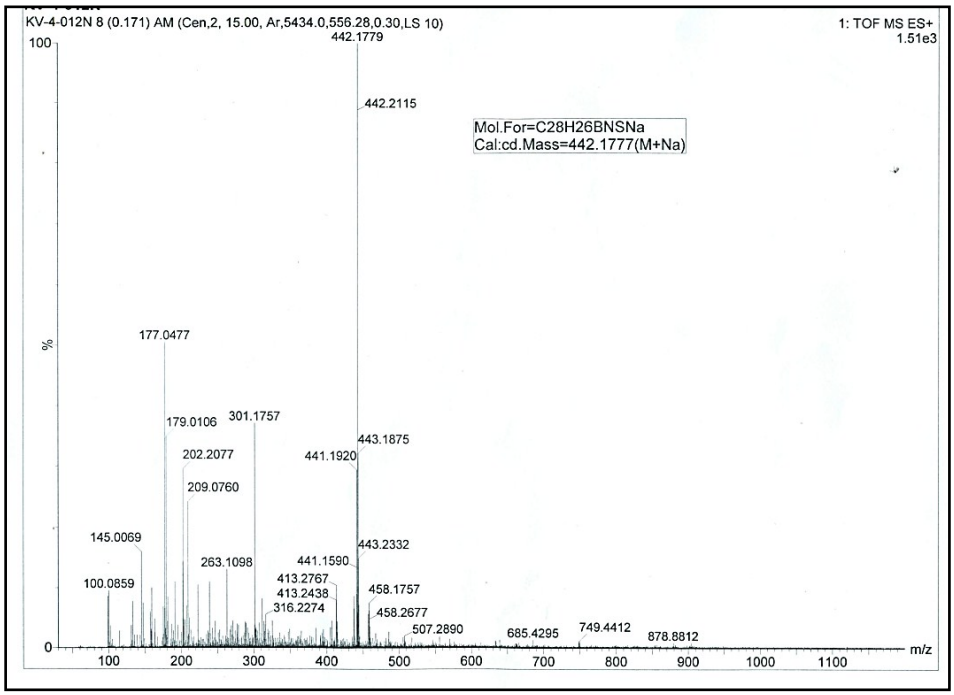

Figure S8: HRMS of compound **2**

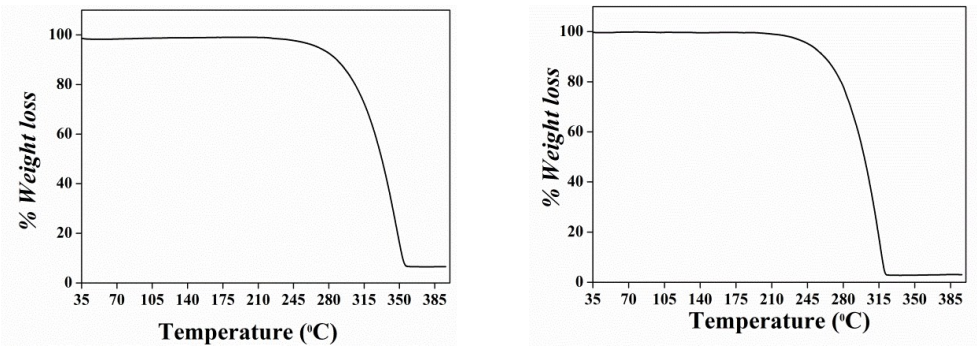

Figure S9: Thermo gravimetric traces of compounds **1** (left) and **2** (right).

Table S1. Crystallographic refinement data of compounds **1** and **2**

	1	**2**
Empirical formula	C30 H30 B N S	C28 H26 B N S
Formula weight	447.42	419.37
Temperature(K)	298(2)	293(2)
Wavelength (Å)	0.71073 Å	0.71073 Å
Crystal system	Monoclinic	Trigonal
Space group	C2/c	R3c
a/ Å	13.789(1)	18.728(6)
b/ Å	19.910(2)	18.728(6)
c/ Å	18.524(1)	34.323(1)
α/°	90.0	90.0
β/°	95.4 (5)	90.0
γ/°	90.0	120.0
V/Å^3	5062.7(9)	10425.8(6)
Crystal size (mm^3)	0.25 x 0.20 x 0.10	0.20 x 0.10 x 0.09
Z	8	18
Density(g cm^{-3})	1.174	1.202
Final R [I>2s(I)] [a], [b]	R1 = 0.0501, wR2 = 0.1507	R1 = 0.0639, wR2 = 0.1221
R (all data)[a], [b]	R1 = 0.0614, wR2 = 0.1589	R1 = 0.1226, wR2 = 0.1568
Highest Peak	0.40	0.18
Deepest Hole	-0.35	-0.22
Collected reflns	40326	17890
Unique reflns	4471	4080
Theta range for data collection	1.8 to 25.0	2.7 to 25.0
Absorption coefficient	0.146	0.155
Goodness-of-fit on F^2	1.081	0.989
CCDC No.	1499042	1499043

[a] $R_1 = \Sigma \left| \left| F_o \right| - \left| F_c \right| \right| / \Sigma \left| F_o \right|$. [b] $wR_2 = [\Sigma\{w(F_o^2 - F_c^2)^2\}/\Sigma\{w(F_o^2)^2\}]^{1/2}$

Table S2. Selected bond lengths (Å), bond angles (°) and dihedral angles (°) for **1** and **2** from the crystal and ground state DFT optimized structures and the below images of compounds shows the atom numbering scheme of **1**, **2** and phenothiazine.

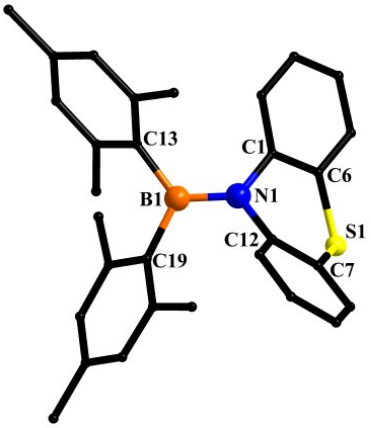

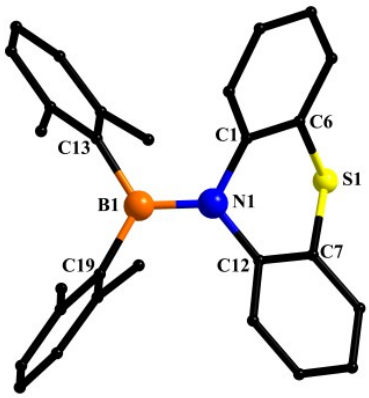

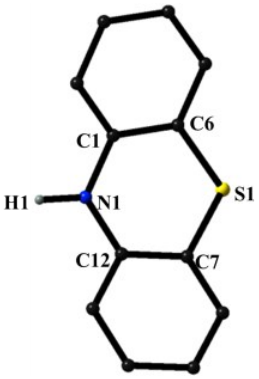

Bond lengths (Å)/Bond angles (°)/torsion angles (°)	**Crystal**		**DFT**		
	1	**2**	**1**	**2**	**Phenothiazine**
B1-N1	1.430(3)	1.445(6)	1.447	1.447	-
B1-C13	1.595(3)	1.602(7)	1.606	1.606	-
B1-C19	1.610(3)	1.592(7)	1.599	1.599	-
N1-C1	1.461(2)	1.435(6)	1.440	1.440	1.441
N1-C12	1.442(2)	1.447(7)	1.449	1.449	1.404
S1-C6	1.764(3)	1.761(5)	1.779	1.779	1.787
S1-C7	1.764(2)	1.756(5)	1.781	1.781	1.786
C7-S1-C6	97.9(1)	97.0(2)	97.5	97.5	99.6
C1-N1-B1	126.3(1)	119.3(4)	120.7	120.7	-
C12-N1-B1	119.5(1)	127.1(4)	125.5	125.5	-
C1-N1-C12	114.0(1)	113.4(4)	113.5	113.5	122.3
C1-N1-H1	-	-	-		113.9
C12-N1-H1	-	-	-		113.9
N1-B1-C19	119.0(1)	120.9(4)	121.5	121.5	
N1-B1-C13	123.1(1)	118.8(4)	119.8	119.8	
C13-B1-C19	117.8(1)	120.3(4)	118.6	118.6	
C1-N1-B1-C19	156.5(2)	-160.7(4)	165.3	165.3	
C1-N1-B1-C13	-23.5(3)	20.6 (6)	-17.0	-17.0	
C12-N1-B1-C13	159.0(2)	-155.0(4)	158.4	158.4	
C12-N1-B1-C19	-20.9(2)	23.7(7)	-19.1	-19.1	

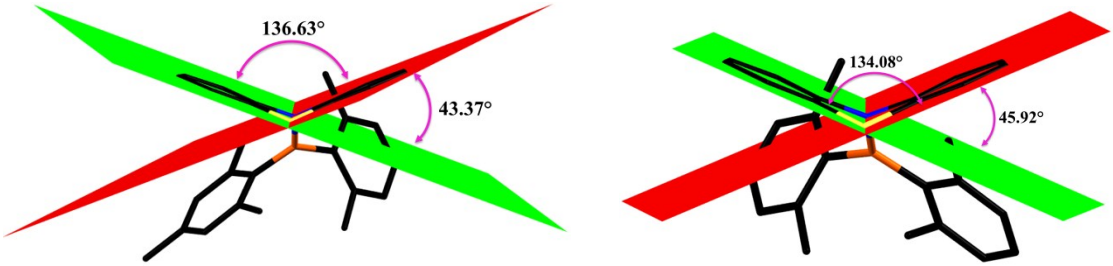

Figure S10: Representation of the folding angle and tilt angle between the two phenyl rings of the phenothiazine moiety in compounds **1** (left) and **2** (right) from the molecular structure. (Folding and Tilt angles were calculated according to the procedure described by Muller el al).[3]

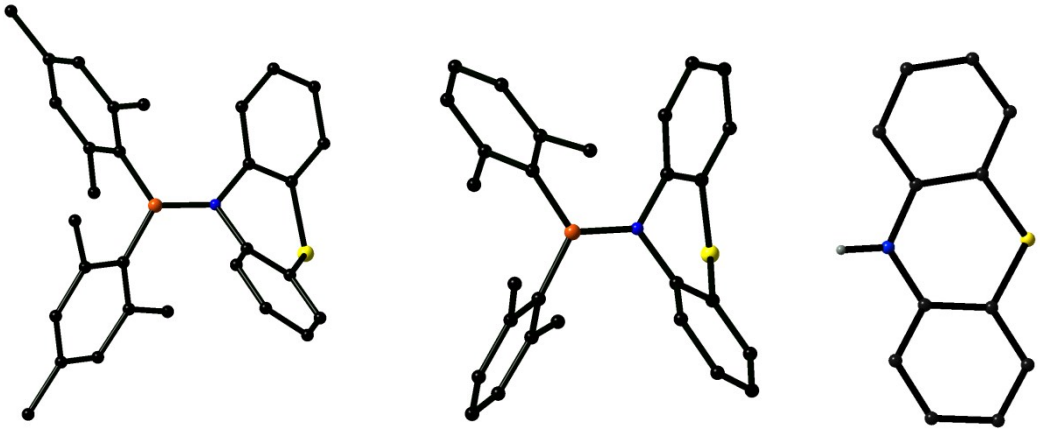

Figure S11: Ground state optimized structure of compounds **1** (left), **2** (middle) and phenothiazine (Atom color codes: C-black, N-blue, B-orange, S-yellow, H-grey, hydrogen atoms connected to all atoms except to nitrogen atom of phenothiazine are removed for clarity).

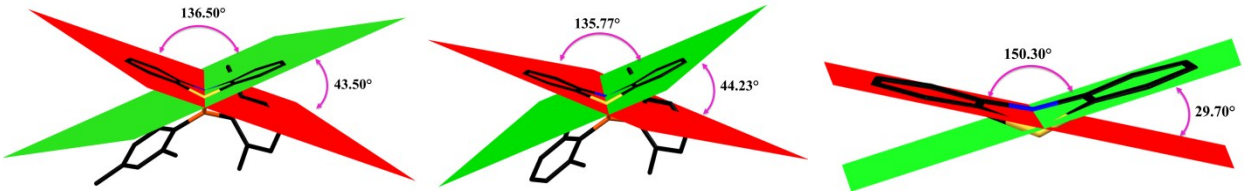

Figure S12: Representation of the folding angle and tilt angle between the two phenyl rings of the phenothiazine moiety in compounds **1** (left), **2** (middle) and phenothiazine (right) from the ground state DFT optimized structures (Atom color codes: C-black, N-blue, B-orange, S-yellow, hydrogen atoms are removed for clarity).

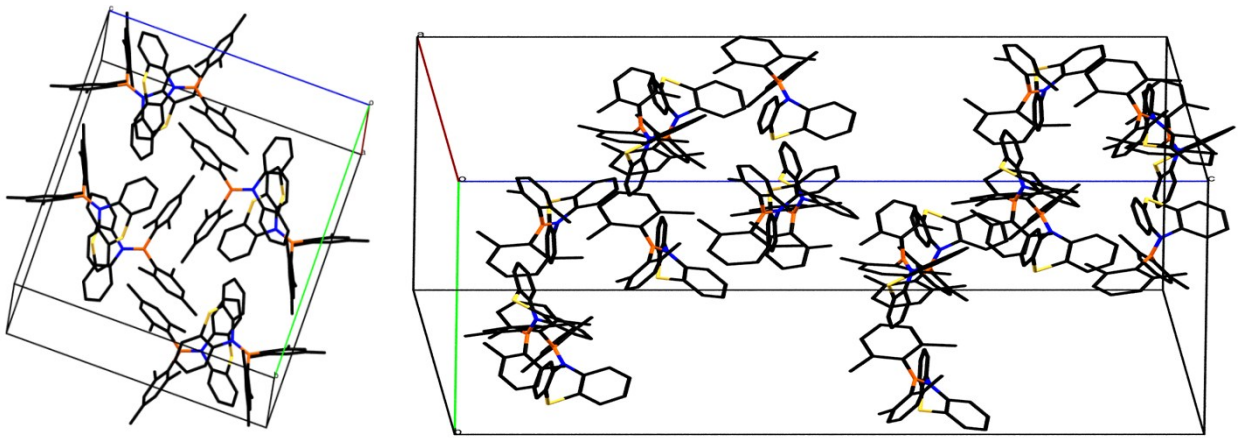

Figure S13: Unit cell packing diagrams of compound **1** (left, Z=18) and **2** (right, Z=18)

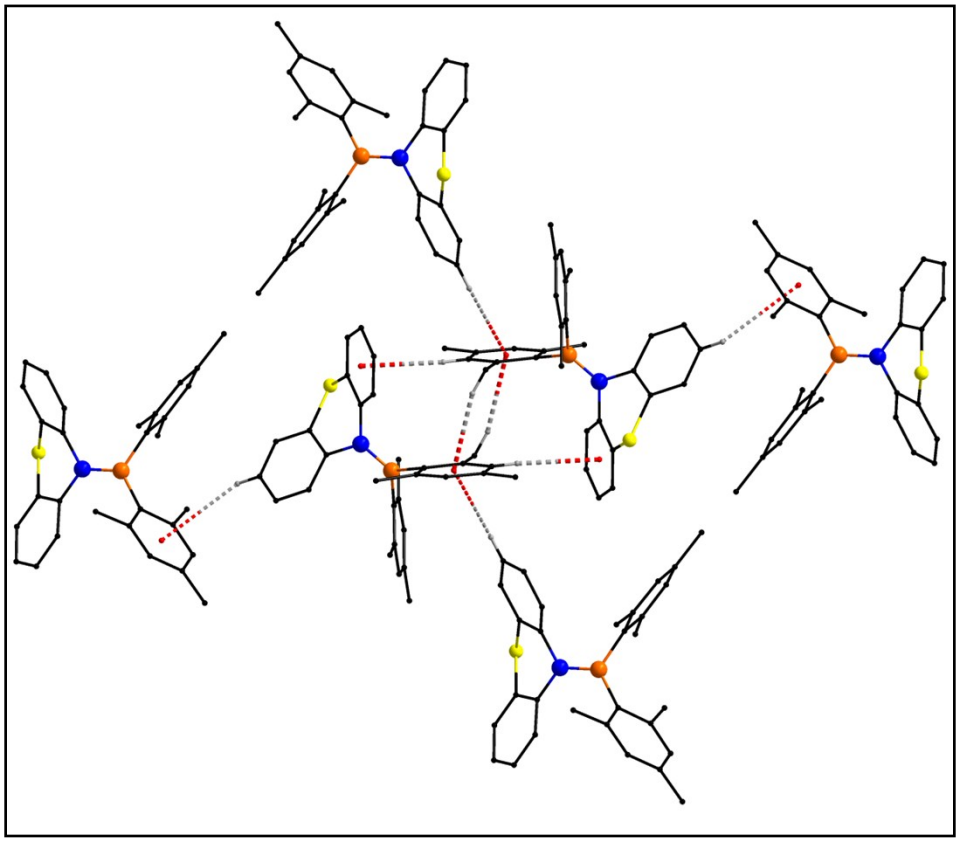

Figure S14: Intermolecular interaction diagram of compound **1** (Atom color codes: C-black, N-blue, B-orange, S-yellow, H-grey, H atoms which are not involved in intermolecular interactions are removed for clarity)

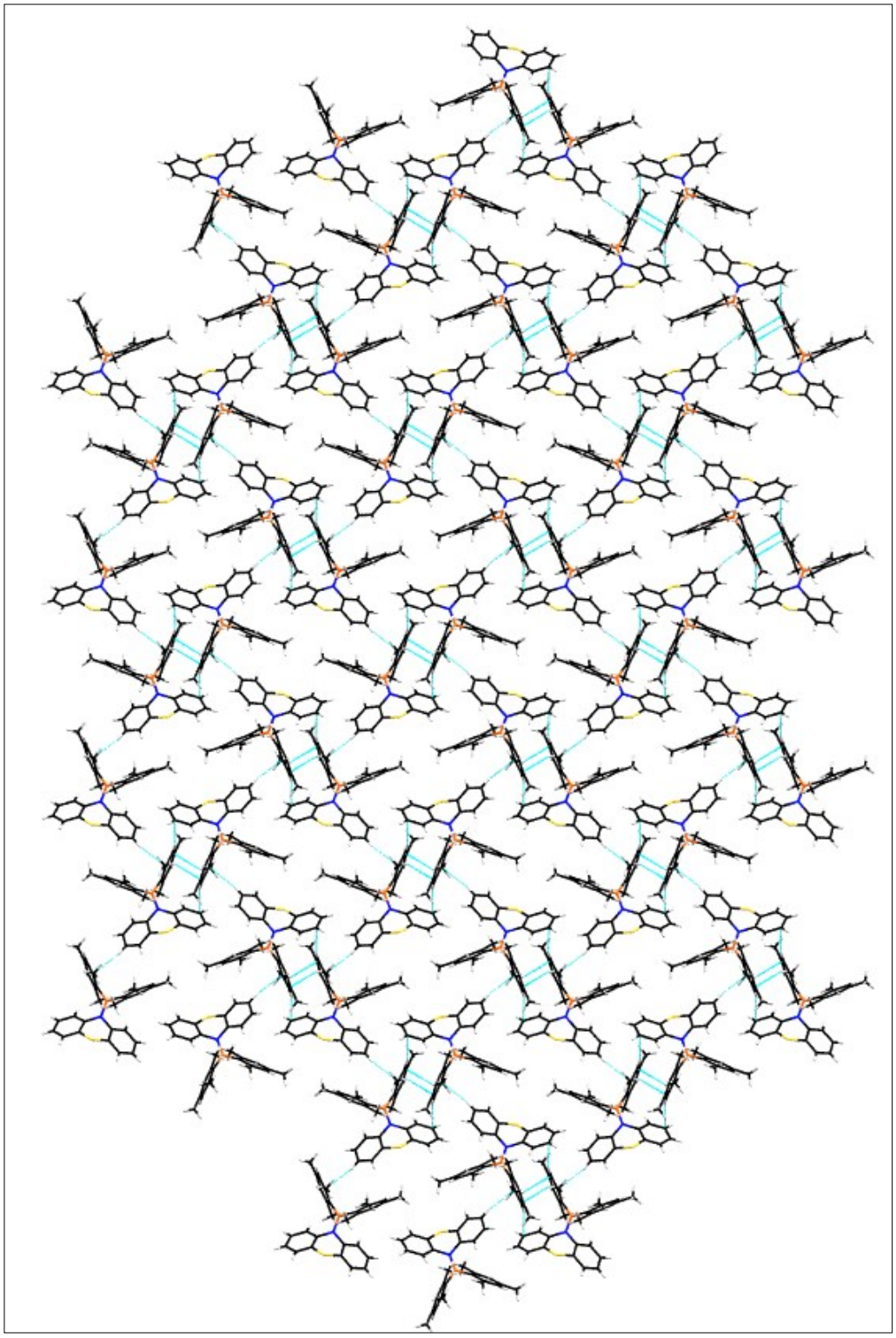

Figure S15: 2D supramolecular structure of **1** formed via CH···π intermolecular interactions shown in Figure S14 (Viewed along a-axis, Atom color codes: C-black, N-blue, B-orange, S-yellow, H-grey).

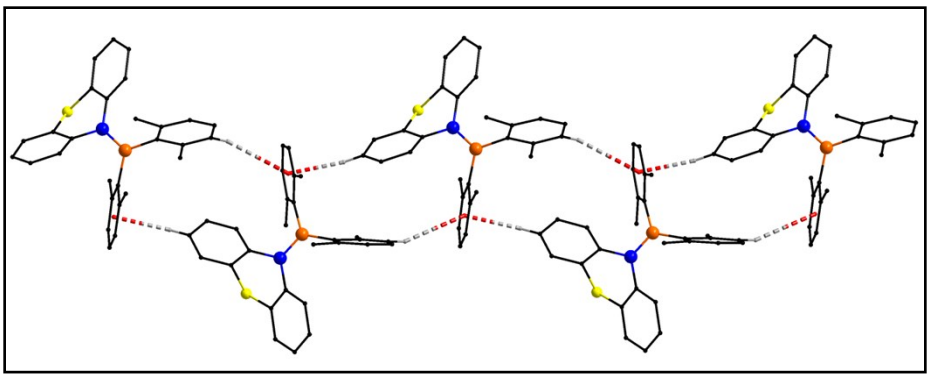

Figure S16: Intermolecular interaction diagrams of compound **2**(Atom color codes: C-black, N-blue, B-orange, S-yellow, H-grey, H atoms which are not involved in intermolecular interactions are removed for clarity)

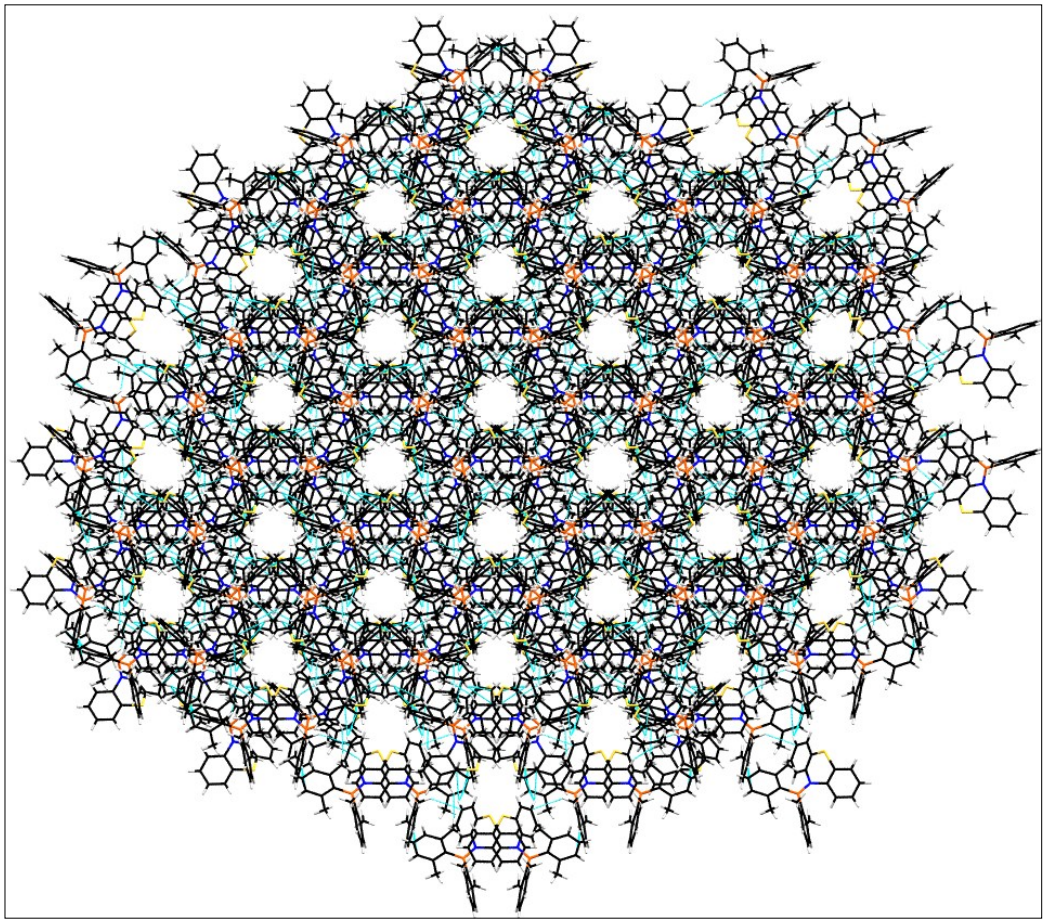

Figure S17: Compound 2 forms 3D supramolecular structure with discrete cylindrical column (diameter of pore is 4.61 Å) via intermolecular CH···π interactions. Atom color codes: C-black, N-blue, B-orange, S-yellow, H-grey). The diameter of the column was calculated by creating a centroid in the cylindrical void by connecting sulphur atoms of phenothiazine moiety of three adjacent molecules in the cylindrical structure.

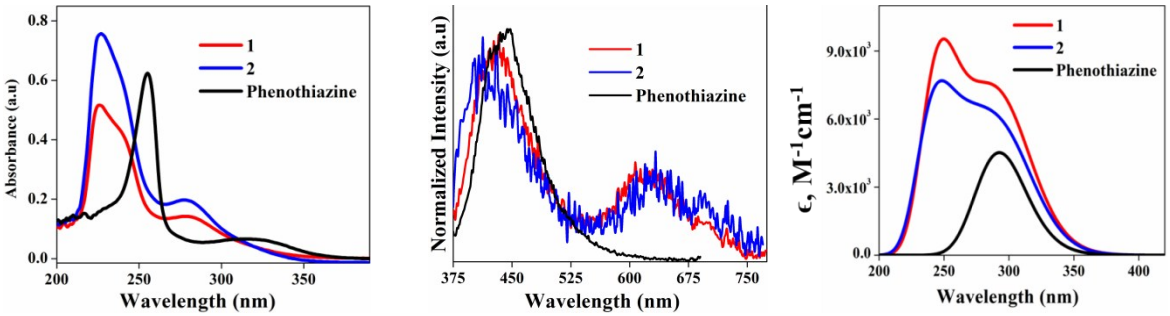

Figure S18: Absorption (left) and emission (middle) spectra of compounds **1**, **2** and phenothiazine in THF solvent (Conc. 10^{-5} M, λ_{ex} = 350 nm). Simulated absorption spectra of **1**, **2** and Phenothiazine in vacuum (right).

Table S3: Photophysical data of compounds **1**, **2** and phenothiazine in THF solvent (Conc. 10^{-5} M, λ_{ex} = 350 nm for emission spectral measurements and 340 nano LED for TRF measurements).

	λ_{abs} (nm) (ϵ, $M^{-1}cm^{-1}$)	λ_{em} (nm)	Life time, τ (ns)			
			τ_1 (A1, %)	τ_2 (A2, %)	τ^a	χ^2
1	226 (51600); 280 (14200)	433	1.40 (80)	5.87 (20)	2.35	1.4
		630	0.42 (8)	5.45 (92)	5.05	1.1
2	227 (75900); 279 (19700)	413	1.89 (84)	7.16 (16)	2.78	1.7
		630	2.48 (6)	8.56 (94)	8.20	1.4
Phenothiazine	255 (62600); 315 (6600)	448	1.26 (93)	6.18 (7)	1.60	1.4

[a] average life time $\tau = \{ (A1\tau_1 + A2\ \tau_2)/100\}$

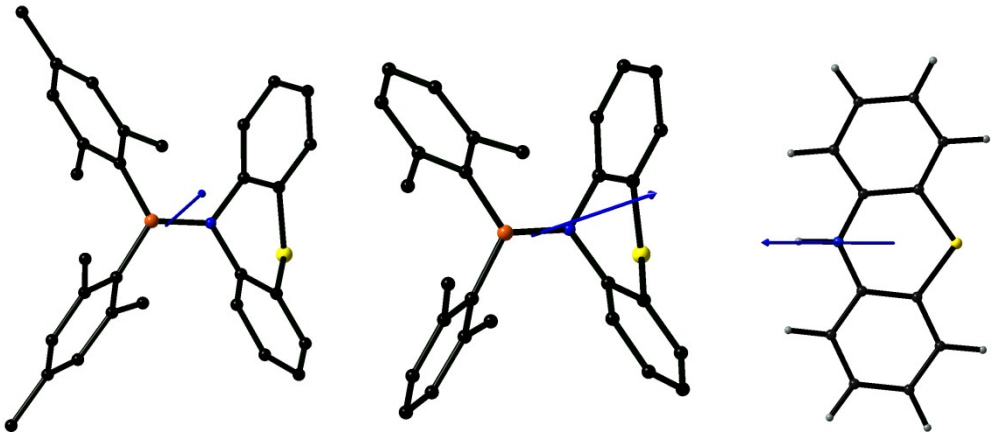

Figure S19: Ground state dipole moment vector from the ground state DFT optimized structures of compounds **1** (left) and **2** (middle) and phenothiazine (Atom color codes: C-black, N-blue, B-orange, S-yellow, H-grey, hydrogen atoms of **1** and **2** are removed for clarity. Ground state dipole moment values are 1.14, 1.30 and 2.26 Debye for **1**, **2** and phenothiazine, respectively).

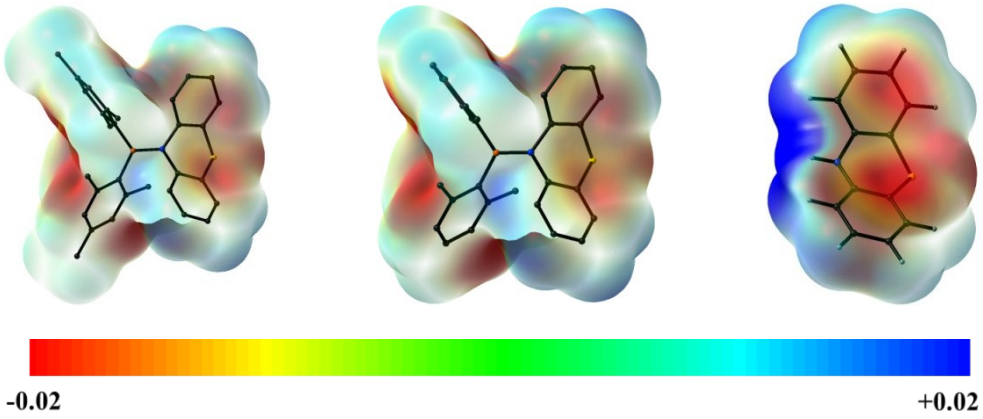

Figure S20: Electrostatic potential energy surface diagrams of **1** (left) and **2** (middle) and phenothiazine (right) from the ground state DFT optimized structures (Atom color codes: C-black, N-blue, B-orange, S-yellow, H-grey, hydrogen atoms of **1** and **2** are removed for clarity, isovalue = 0.0004).

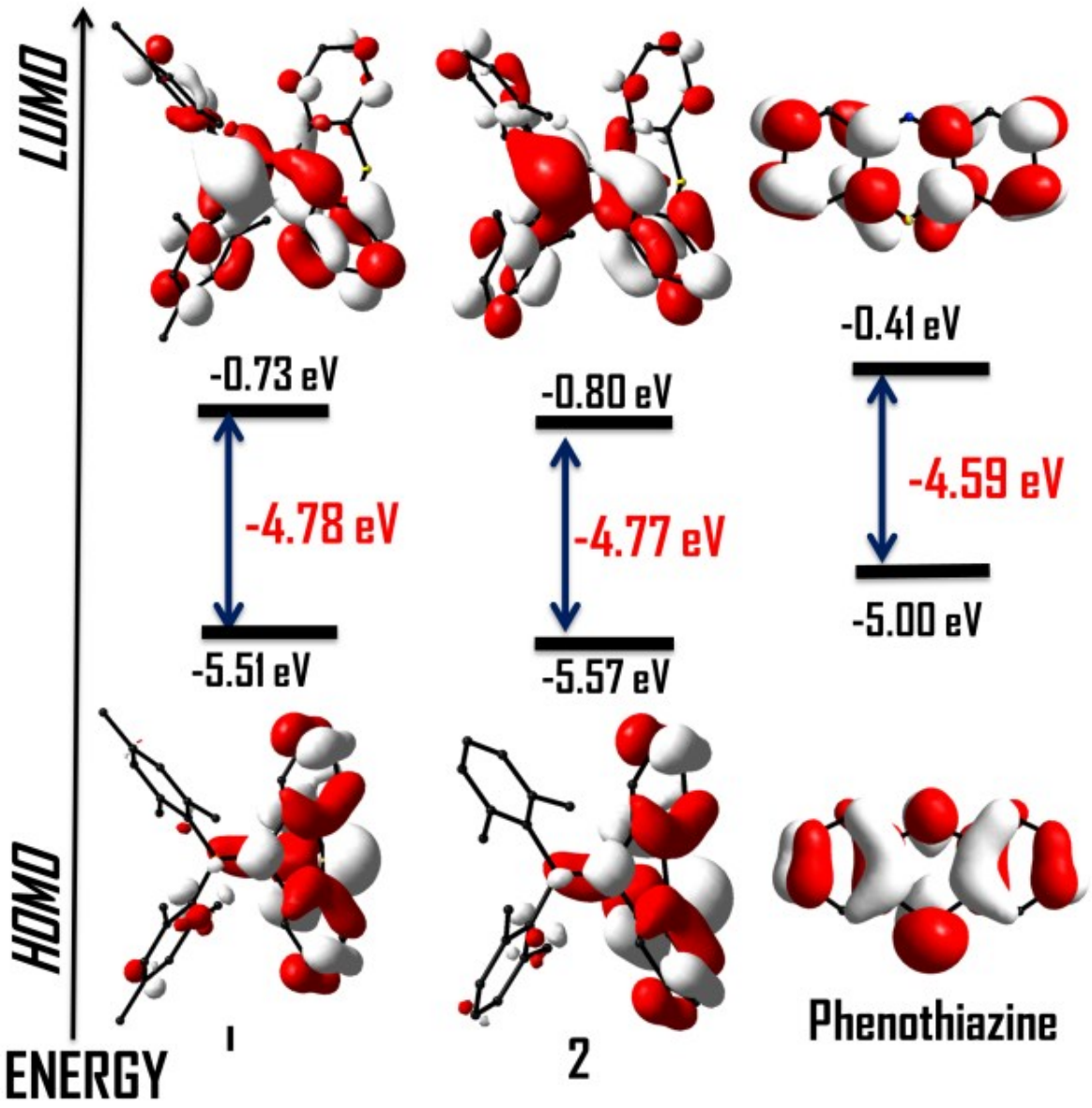

Figure S21: Frontier molecular orbital surfaces energy level diagram of compounds **1**, **2** and phenothiazine (energies are not to the scale, Hydrogen atoms are omitted for clarity).

Table S4: Summary of dominant electronic transitions of compounds **1, 2** and Phenothiazine obtained from TD-DFT calculations

Compound	Excited State	E/eV	E/nm	f	Dominant transitions (percent contribution)
1	1	4.109	301.7	0.112	HOMO ->LUMO (95%)
	2	4.401	281.7	0.027	HOMO ->LUMO+2 (66%)
	3	4.446	278.8	0.039	HOMO-1 ->LUMO (72%)
	6	4.600	269.5	0.018	HOMO-3 ->LUMO (91%)
	7	4.707	263.4	0.022	HOMO ->LUMO+3 (72%)
2	1	4.101	302.3	0.093	HOMO ->LUMO (95%)
	2	4.410	281.1	0.027	HOMO ->LUMO+2 (66%)
	3	4.506	275.1	0.034	HOMO ->LUMO+1 (36%)
	5	4.607	269.08	0.021	HOMO-2 ->LUMO (53%)
	6	4.715	270.0	0.016	HOMO ->LUMO+3 (74%)
Phenothiazine	2	4.199	295.2	0.024	HOMO ->LUMO+1 (94%)
	3	4.248	291.8	0.088	HOMO ->LUMO+2 (87%)
	4	4.988	248.5	0.048	HOMO ->LUMO+4 (89%)
	5	5.145	240.9	0.025	HOMO ->LUMO+4 (84%)
	6	5.154	240.5	0.411	HOMO-1 ->LUMO (84%)

Table S5: Solid state luminescence properties of compounds **1** and **2** (λ_{ex} = 350 nm for emission spectral measurements and 340 nano-LED for TRF measurements).

	λ_{em} (nm)	Φ_F (%)	Life time, τ (ns)				k_r x 10^6 $(s^{-1})^b$	k_{nr} x 10^6 $(s^{-1})^b$
			τ_1 (A1, %)	τ_2 (A2, %)	τ^a	χ^2		
1	485	20.01	5.11 (14)	5.07 (86)	5.08	1.2	39.39	157.46
2	513	38.17	0.34 (4)	9.26 (96)	8.90	1.1	42.89	69.47

[a] average life time, $\tau = \{ (A1\tau_1 + A2\ \tau_2)/100\}$; [b] following equations have been used for the calculation of k_r and k_{nr}; $\{ \phi_F = k_r/(k_r+k_{nr})\}$ and $_{\{}\tau = 1/(k_r+k_{nr})\}$, where ϕ_F is the fluorescence quantum yield, τ is the average life time and k_r and k_{nr} are the radiative non-radiative (k_{nr}) decay rate constants, respectievely.[4]

Aggregation Induced Emission studies

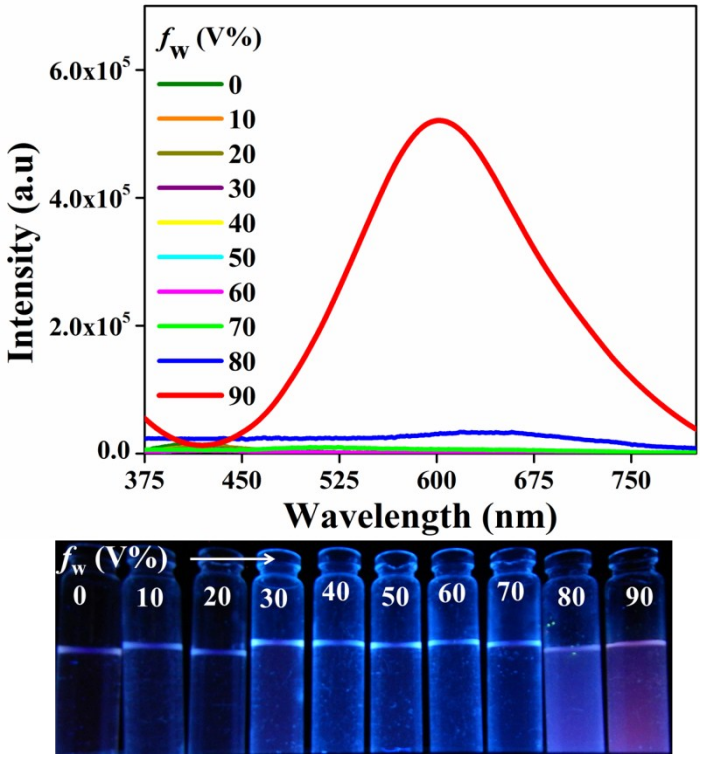

Figure S22. PL spectra of **2** in THF/water mixtures with different water fraction, f_w (V %) (Conc. 100 μM, λex = 350 nm) and the images of compound in THF with increasing water fraction taken under UV light illumination (λ= 280- 365 nm).

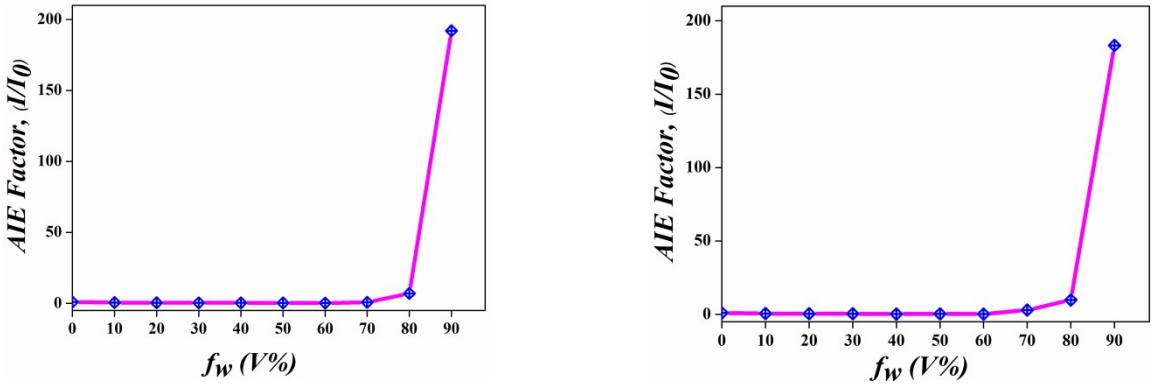

Figure S23: Relative luminescence intensity (I/I_0) as a function of volume of water fraction (f_w (V %) for compounds **1** (left) and **2** (right).

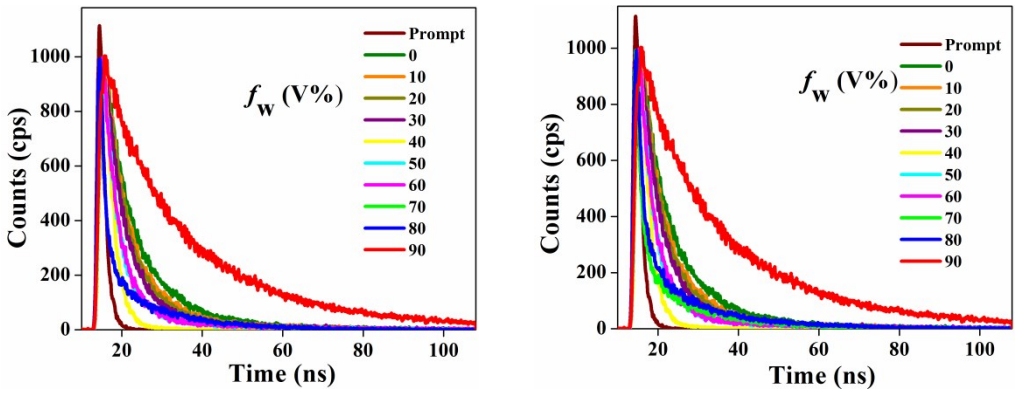

Figure S24: Time resolved fluorescence decay profile of compounds **1** (left) and **2** (right), in THF solvent with different water fraction, f_w (V %) (Conc. 10^{-4} M, λ_{ex} = 340 nano-LED).

Table S6: Time resolved fluorescence decay data for compounds **1** and **2** in THF solvent with 0 and 90 % water fraction, f_w (V%) (Conc. 10^{-4} M, λ_{ex} = 340 nano LED).

	f_w(V%)	τ_1, ns (A1, %)	τ_2, ns (A2, %)	τ^a (ns)	χ^2
1	0	0.73 (11)	4.51 (89)	4.09	1.1
	90	1.02 (7)	11.76 (93)	11.00	1.2
2	0	2.02 (53)	9.74 (47)	5.65	1.0
	90	1.28 (11)	9.23 (89)	8.36	1.0

[a] average life time, $\tau = \{ (A1\tau_1 + A2\ \tau_2)/100\}$

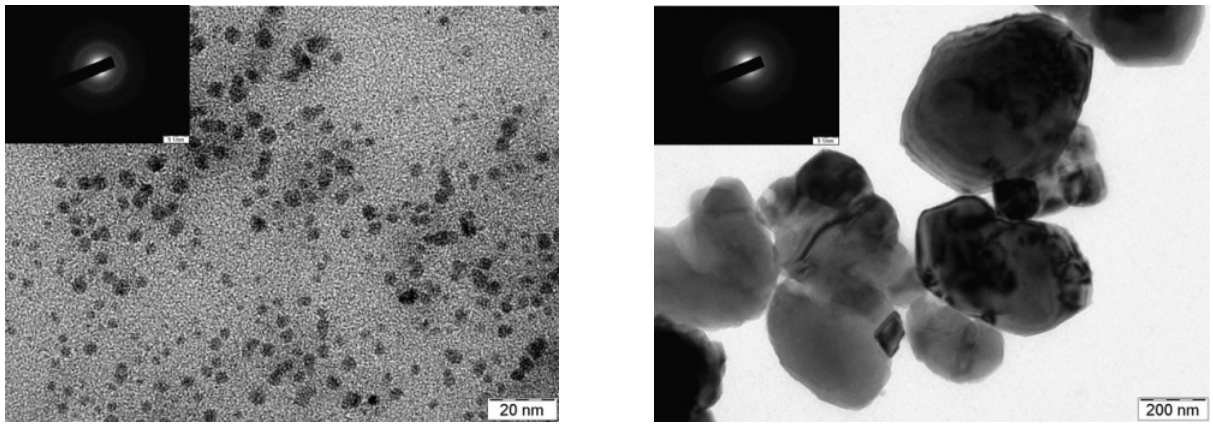

Figure S25: Transmission electron microscopy (TEM) images of the nanoaggregates formed in 1:9 THF-water mixture of compounds **1** (left) and **2** (right), inset shows the corresponding SAED pattern (Conc. 10^{-4} M).

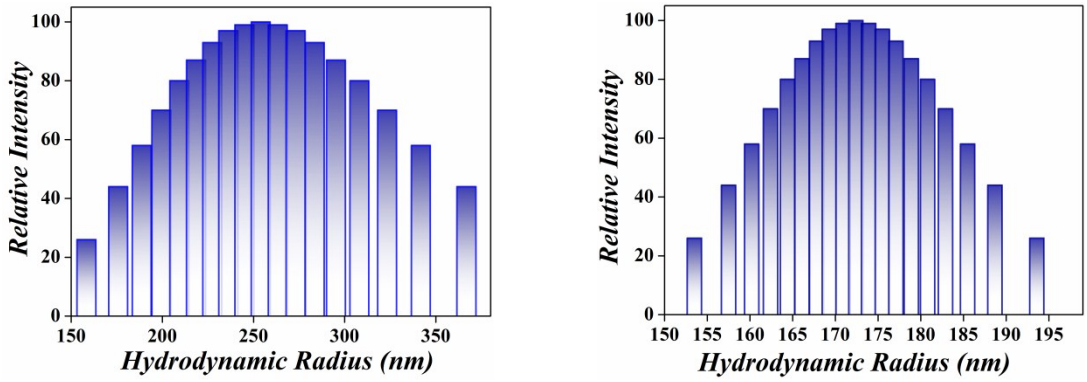

Figure S26: Particle size distribution pattern of the nanoaggregates formed in 1:9 THF-water mixture of compounds **1** (left) and **2** (right) obtained from dynamic light scattering (DLS) measurements (Conc. 10^{-4} M) Average hydrodynamic radius for **1** and **2** are 254 nm and 172 nm, respectively.

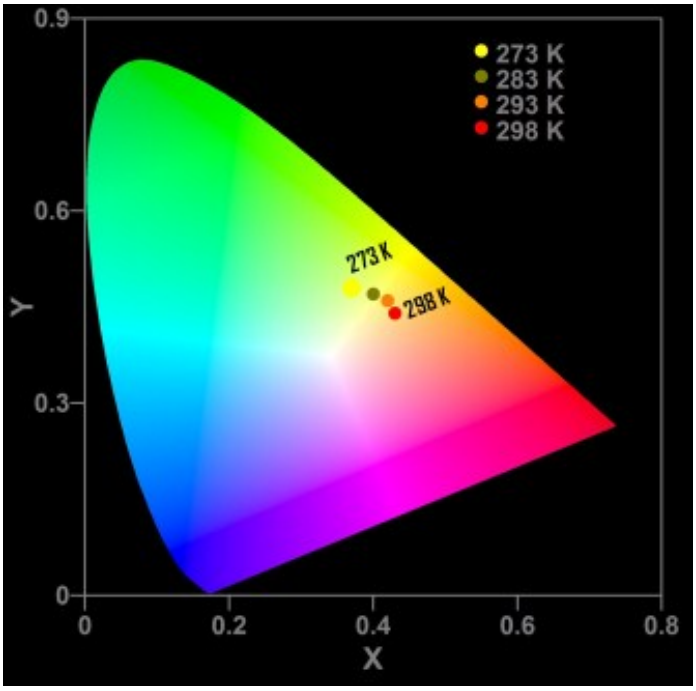

Figure S27: Calculated PL color coordinates for temperature dependent emission studies of compound **1** in the CIE 1931 chromaticity diagram (bottom).[5]

Table S7: Temperature dependent emission data of compound **1** in 1:9 THF: water Mixture (Conc. 10^{-4} M, λ_{ex} = 350 nm for emission spectral measurements and 340 nano LED for TRF measurements)

Temperature (K)	λ_{em} (nm)	Life time, τ (ns)				Calculated emission colour coordinates (x,y) in CIE 1931 chromaticity diagram.[5]
		τ_1 (A1, %)	τ_2 (A2, %)	τ^a	χ^2	
298	585	1.02 (7)	11.76 (93)	11.00	1.2	0.43, 0.44
293	574	0.88 (5)	12.50 (95)	11.87	1.1	0.42, 0.46
283	567	2.04 (3)	13.28 (97)	12.94	1.1	0.40, 0.47
273	551	3.65 (4)	13.60 (96)	13.20	1.0	0.37, 0.48

[a] average life time, $\tau = \{ (A1\tau_1 + A2\ \tau_2)/100\}$

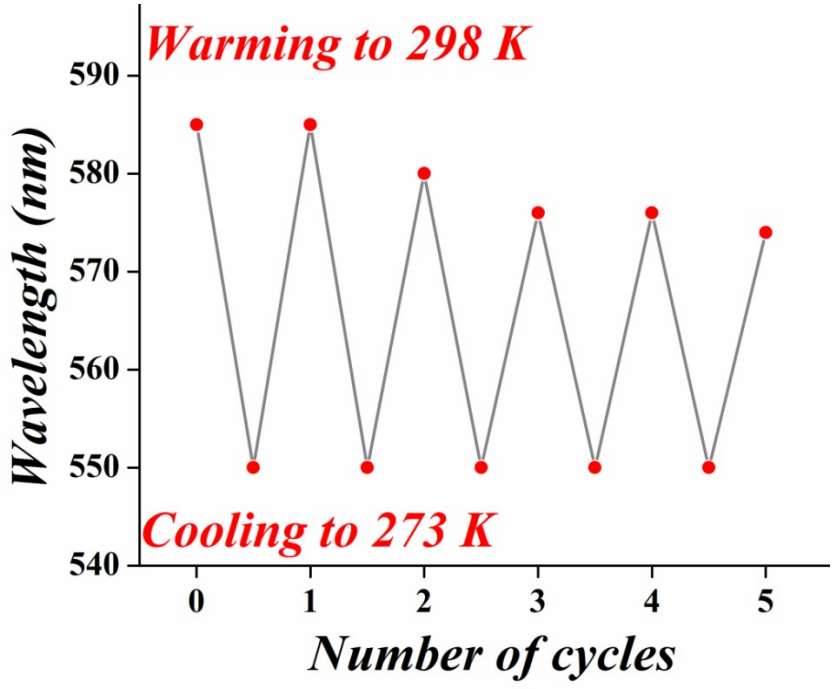

Figure S28: Change of emission wavelengh of **1** in 1:9 THF-water mixture upon repeated cycles of cooling (273 K) and warming (298 K). The reversibility of temperature dependent PL characteristics of nano-aggregates of **1** was measured with cooling (273 K) and warming (298 K) of the the sample. The warming of the cooled sample initially gave an emission centered at ~ 585 nm, which is exactly matches with the emission of nano-aggregates of **1** at RT prior to cooling. After two cycles the emission at 298 K was slightly blue shifted (~ 580 nm) and stabilized in further cycles of cooling and warming. This might due to the formation of strong intermolecular interactions in the aggregates.

Mechanochromic Luminescence

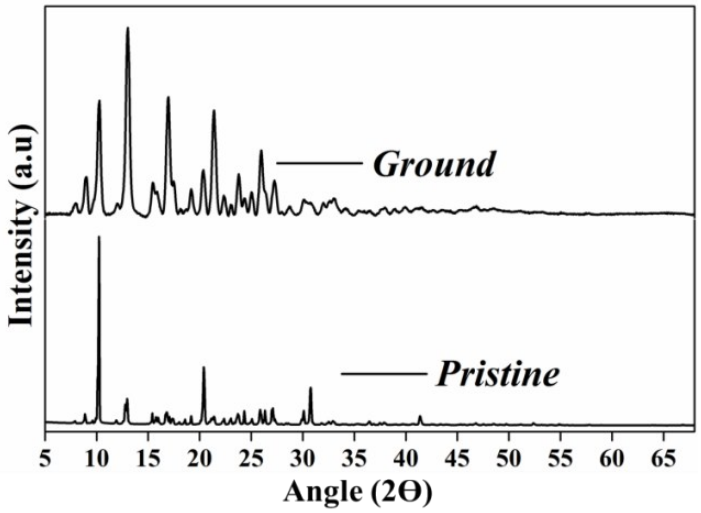

Figure S29: PXRD pattern of pristine and ground samples of **1** (right).

Table S8: Mechanochromic luminescence properties of compound **1** (λ_{ex} = 350 nm for emission spectral measurements and 340 nano-LED for TRF measurements).

	λ_{em} (nm)	Φ_F (%)	Life time, τ (ns)			
			τ_1 (A1, %)	τ_2 (A2, %)	τ^a	χ^2
1 (Pristine)	485	20.01	5.11 (14)	5.07 (86)	5.08	1.2
1 (Ground)	505	24.12	7.49 (47)	11.12 (53)	9.41	1.07

[a] average life time, $\tau = \{ (A1\tau_1 + A2\ \tau_2)/100\}$

Triboluminescence measurements

Images and videos for triboluminescence of compound **2** were captured by crushing the crystals using a stainless spatula.

Triboluminescence emission spectral measurements were carried out in a high resolution multichannel fluorescence spectrophotometer aided with a LN_2- cooled CCD (HORIBA). Emission signals were collected through optical fibers which are connected at the bottom of the sample holder. Optical fibers were terminated in a linear array were placed in a telescopic arrangement at the entrance slit of the spectrometer. The spectrometer entrance slit was adjusted to 200 μM and grating was 1200 groves per mm. Compound was grinded continuously in a glass sample tube manually using a stainless steel spatula the emission signals were collected with 5 Sec acquisition time. Measurements were carried out at room temperature (25 °C). The emission spectrum was plotted after subtracting from the background measurements.

References

1. (a) a) a) SAINT-NT, Version 6.04; Bruker AXS: Madison, WI, 2001; b) SHELXTL-NT, Version 6.10; Bruker AXS: Madison, WI, 2000.
2. a) A. D. Becke, *J. Chem. Phys.* 1993, **98**, 5648-5652; b) Gaussian 09, Revision A.02, M. J. Frisch, G. W. Trucks, H. B. Schlegel, G. E. Scuseria, M. A. Robb, J. R. Cheeseman, G. Scalmani, V. Barone, B. Mennucci, G. A. Petersson, H. Nakatsuji, M. Caricato, X. Li, H. P. Hratchian, A. F. Izmaylov, J. Bloino, G. Zheng, J. L. Sonnenberg, M. Hada, M. Ehara, K. Toyota, R. Fukuda, J. Hasegawa, M. Ishida, T. Nakajima, Y. Honda, O. Kitao, H. Nakai, T. Vreven, J. A. Montgomery, Jr., J. E. Peralta, F. Ogliaro, M. Bearpark, J. J. Heyd, E. Brothers, K. N. Kudin, V. N. Staroverov, R. Kobayashi, J. Normand, K. Raghavachari, A. Rendell, J. C. Burant, S. S. Iyengar, J. Tomasi, M. Cossi, N. Rega, J. M. Millam, M. Klene, J. E. Knox, J. B. Cross, V. Bakken, C. Adamo, J. Jaramillo, R. Gomperts, R. E. Stratmann, O. Yazyev, A. J. Austin, R. Cammi, C. Pomelli, J. W. Ochterski, R. L. Martin, K. Morokuma, V. G. Zakrzewski, G. A. Voth, P. Salvador, J. J. Dannenberg, S. Dapprich, A. D. Daniels, O. Farkas, J. B. Foresman, J. V. Ortiz, J. Cioslowski, and D. J. Fox, Gaussian, Inc., Wallingford CT, 2009; c) A. D. Becke, *Phys. Rev. A.* 1988, **38**, 3098-3100; d) C. Lee, W. Yang, R. G. Parr, *Phys. Rev. B.* 1988, **37**, 785-789.
3. M. Hauck, M. Stolte, J. Schönhaber, H.-G. Kuball, T. J. J. Müller, *Chem. Eur. J.* 2011, **17**, 9984-9998.
4. B. Kupcewicz and M. Małecka, *Cryst. Growth Des.*, 2015, **15**, 3893-3904.
5. CIE, Commission internationale de l'Eclairage proceedings, 1931, Cambridge University Press, Cambridge, 1932; (b) L. A. Jones, *J. Opt.Soc. Am.* 1943, **33**, 534.